Supporting Information

Photo-responsive circularly polarized long-lived fluorescence in chiral liquid crystals via tunable stepwise energy transfer

Xincan Wang,[a] Jiani Wang,[a] Sha Huang,[a] Yongjie Yuan,[*a] and Hailiang Zhang[*a]

[a]Key Laboratory of Polymeric Materials and Application Technology of Hunan Province, Key Laboratory of Advanced Organic Functional Materials of Colleges and Universities of Hunan Province, College of Chemistry, Xiangtan University, Xiangtan 411105, Hunan Province, China.

* Corresponding author

E-mail: hailiangzhang@xtu.edu.cn; yuanyongjie@xtu.edu.cn;

Materials

Dibenzofuran (98%), 4-methoxybenzoyl chloride (97%), 6-bromo-1-hexanol (97%), anhydrous aluminium chloride (99%), boron tribromide (99.9%), cholesteryl chloroformate (98%), 4-dimethylaminopyridine (DMAP, 98%), N,N-dimethyl-formamide (≥99.9%), pyridine (≥99.9%), sodium chloride (99.9%), potassium carbonate (99%), potassium iodide (99%), cholesteryl chloroformate (98%), 2,3,3-

trimethyl-3H-indole (98%), 5-nitrosalicylaldehyde (98%), iodomethane (99.5%), sodium hydroxide (99.9%) were purchased from Energy Chemical Co. Ltd. Dichloromethane (AR), tetrahydrofuran (AR), 1,6-dibromohexane (AR), methanol (AR), petroleum ether (AR), acetonitrile (AR), ethanol (AR), and hydrochloric acid (AR) were purchased from Huihong Reagent Co., Ltd. All materials were used as received without any further purification.

Measurements and characterizations

The ^{1}H NMR and ^{13}C NMR spectra of intermediates and final products were recorded using a Bruker ARX 400 MHz spectrometer. The molecular weights of the intermediates and final products were determined with a Bruker Biflex III MALDI-TOF spectrometer. Phase textures and their changes during the cooling process were observed using a Leica DM 4500 P polarizing microscope. The phase structure of the samples was analyzed by high-flux X-ray diffraction (SAXSess mc^2, Anton Paar), equipped with a Kratky block collimation system and a GE ID3003 sealed-tube X-ray generator (Cu Kα). UV-Vis absorption spectra were obtained using an Agilent Cary 100 spectrometer. Prompt emission spectra were recorded on a PTI Qm 40 luminescence spectrometer. Delayed emission spectra were recorded on a FLS-1000 photoluminescence spectrometer. UV-Vis diffuse reflectance spectra were measured with a Shimadzu Solid Spec-3700 spectrometer, equipped with an integrating sphere. Luminescence lifetimes were measured with a HORIBA QuantaMaster 8000. Circular

dichroism (CD) spectra were recorded using a JASCO J-810 spectrometer, and circularly polarized luminescence (CPL) spectra were obtained with a JASCO CPL-300 instrument. Solid-state luminescence quantum yields were measured with a Quantaurus-QY (C11347, Hamamatsu). In the photo response test, both the 365 nm and 470 nm light sources have a power of 30 W.

Synthesis of SP

The synthetic method for SP is shown in Figure S1, and the detailed process is described as follows.

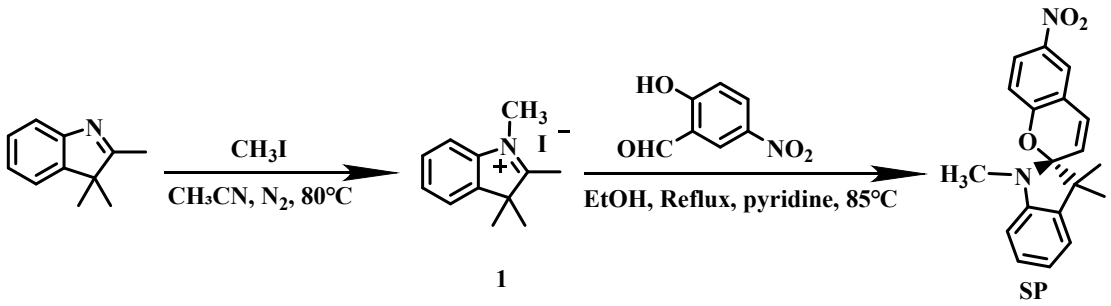

Figure S1. The synthetic route of SP.

Synthesis of compound (1). 2,3,3-Trimethyl-3H-indole (8.0 g, 50.3 mmol), iodomethane (8.9 g, 62.7 mmol), and 25 mL of acetonitrile were successively added to a 250 mL round-bottom flask. The mixture was stirred at 80°C for 16 hours under a nitrogen atmosphere, resulting in the precipitation of a large amount of rose-red solid. Upon completion of the reaction, the solution was allowed to cool naturally to room temperature. The precipitate was then collected by suction filtration, washed with petroleum ether three times, and dried. Finally, 8.3 g of the pure product was obtained,

corresponding to a yield of 93.3%. ^{1}H NMR (400 MHz, $CDCl_3$, δ): 1.25-1.68 (s, 6H, -CH_3), 2.49 (s, 3H, -CH_3), 3.11 (s, 3H, -CH_3), 7.41-7.24 (m, 2H, Ph-H), 7.57 (dd, J=12.0, 4.1 Hz, 1H, Ph-H), 7.66 (m, 1H, Ph-H). ^{13}C NMR (100 MHz, $CDCl_3$, δ) 17.20, 23.19, 29.72, 37.23, 115.11, 123.14, 129.62, 130.32, 141.32, 141.87, 195.91. Mass Spectrometry (MS) (m/z) $[M]^+$ Caled for $C_{12}H_{16}N$, 174.10; found 174.10 $[M]^+$.

Synthesis of SP. Compound (1) (5.0 g, 28.7 mmol), 5-nitrosalicylaldehyde (5.3 g, 31.6 mmol), 50 mL of ethanol, and a small amount of pyridine were successively added to a 250 mL round-bottom flask, and the mixture was stirred at 65°C for 12 hours. Upon completion of the reaction, the solution was allowed to cool naturally to room temperature. The solvent (ethanol) was then removed using a rotary evaporator. The solid crude product was transferred to a beaker and washed sequentially three times with dilute hydrochloric acid and sodium hydroxide aqueous solutions. Finally, the product was collected, dried, and 8.4 g of pure product was obtained, corresponding to a yield of 90.8%. ^{1}H NMR (400 MHz, $CDCl_3$, δ): 1.18 (s, 3H, -CH_3), 1.28 (s, 3H, -CH_3), 2.73 (s, 3H, -CH_3), 5.85 (d, J=10.4 Hz, 1H, -CH=CH-), 6.55 (d, J=7.8 Hz, 1H, Ph-H), 6.76 (d, J=8.6 Hz, 1H, -CH=CH-), 6.95-6.84 (m, 2H, Ph-H), 7.08 (d, J=7.2 Hz, 1H, Ph-H), 7.20 (t, J=7.7 Hz, 1H, Ph-H), 7.99 (s, 1H, Ph-H), 8.02 (d, J=2.8 Hz, 1H, Ph-H). ^{13}C NMR (100 MHz, $CDCl_3$, δ) 19.95, 25.90, 28.89, 52.30, 106.40, 107.09, 115.51, 118.68, 119.78, 121.60, 121.67, 122.70, 125.90, 127.87, 128.30, 136.12, 140.94, 147.71, 159.85. Mass Spectrometry (MS) (m/z) $[M]^+$ Calcd for $C_{19}H_{18}N_2O_3$, 322.45; found, 322.45 $[M]^+$.

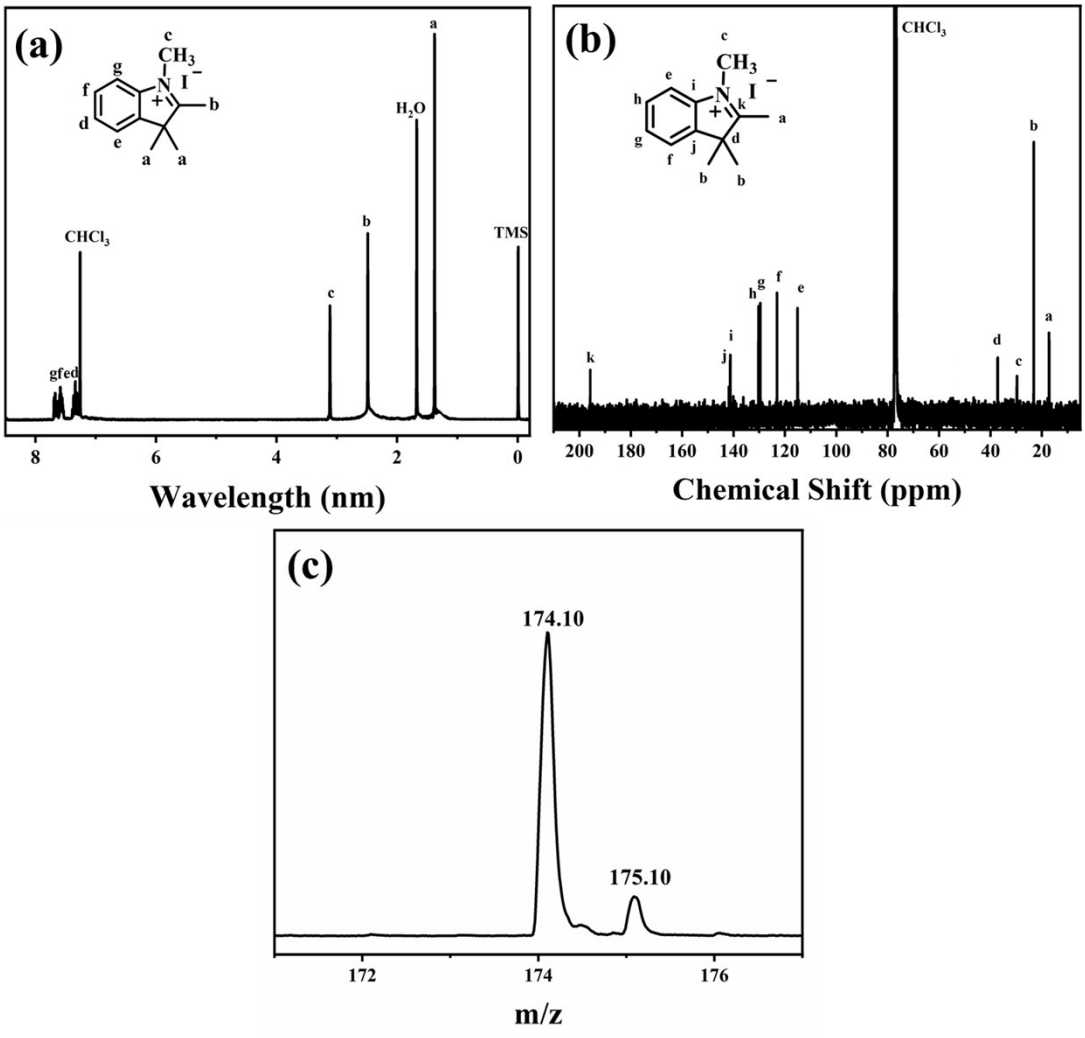

Figure S2. (a) ^{1}H NMR and (b) ^{13}C NMR spectra of compound (1) in $CDCl_3$. (c) MS spectrum of compound (1) in $CHCl_3$.

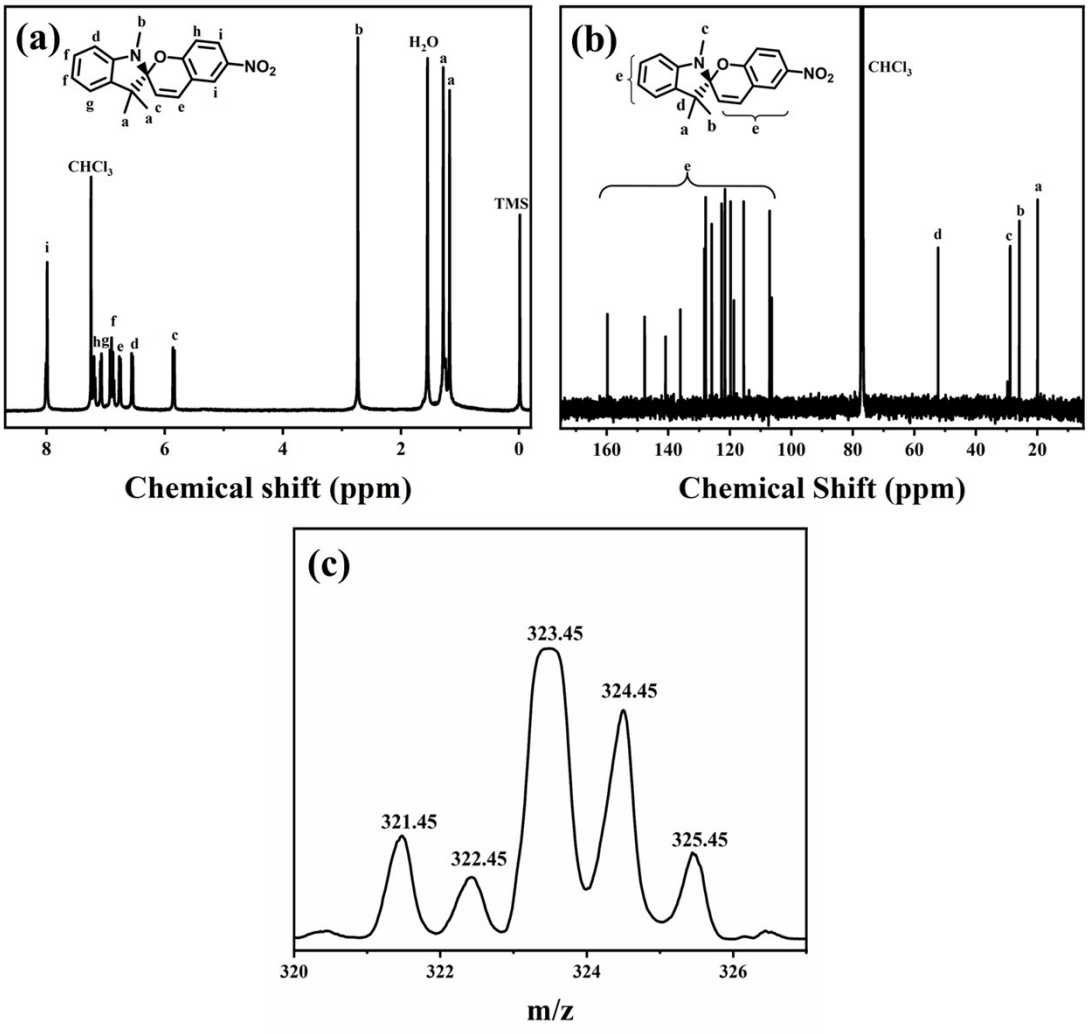

Figure S3. (a) ^{1}H NMR and (b) ^{13}C NMR spectra of SP in $CDCl_3$. (c) MS spectrum of SP in $CHCl_3$.

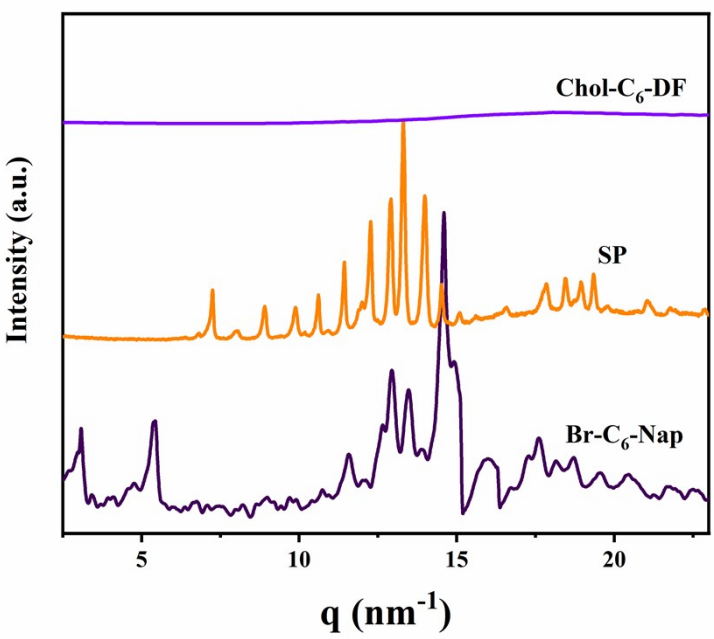

Figure S4. The SAXS curves of Chol-C_6-DF, SP, and Br-C_6-Nap at 30℃.

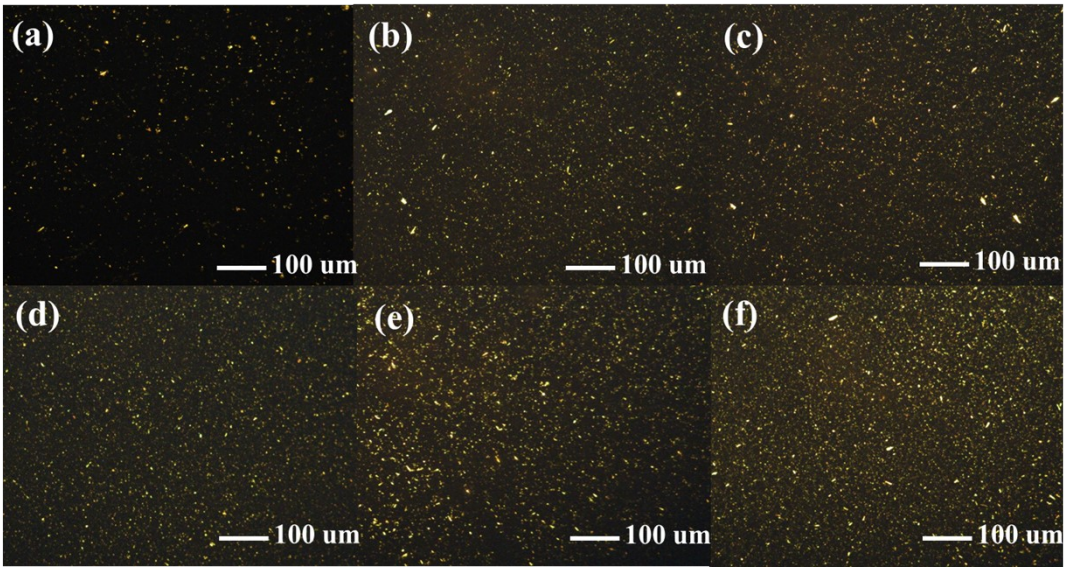

Figure S5. POM images of DF-Nap (a) and DF-Nap-SP(n) with different doping amount of SP, (b) DF-Nap-SP(0.2), (c) DF-Nap-SP(0.4), (d) DF-Nap-SP(0.6), (e) DF-Nap-SP(0.8), and (f) DF-Nap-SP(1), respectively (120℃, magnification=200x).

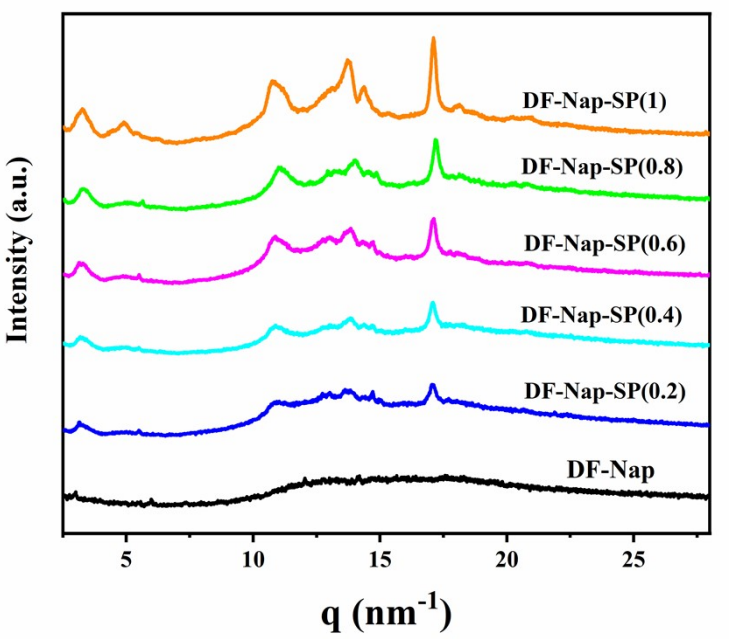

Figure S6. The SAXS spectra of DF-Nap and DF-Nap-SP(n) at 30℃.

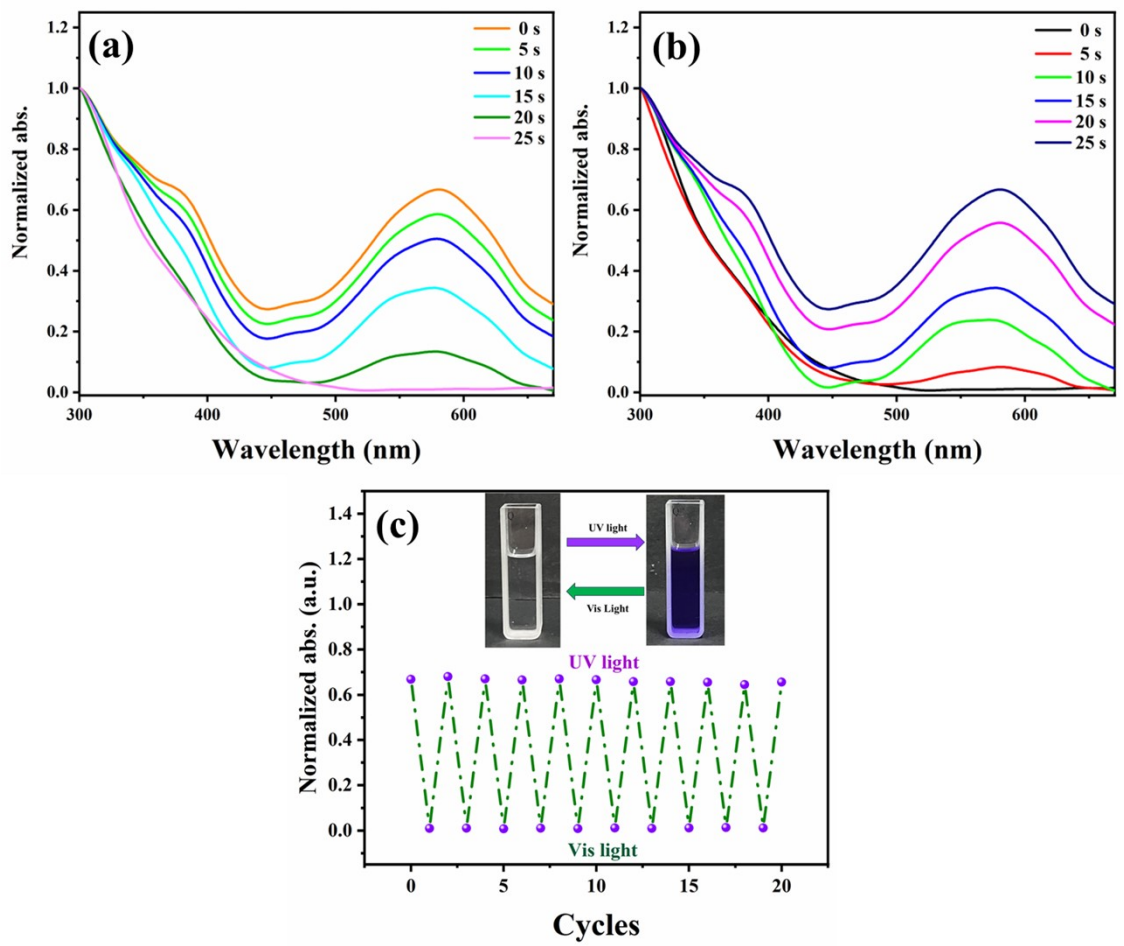

Figure S7. UV-vis absorption spectra of SP in $CHCl_3$ solutions (c=0.1 mg/mL) under irradiation with 365 nm light (a) and subsequent exposure to 470 nm light (b). (c) Change in absorption intensity of SP at 580 nm upon alternating illumination with 365 nm and 470 nm light. The inset images show the reversible color change of SP in $CHCl_3$ solutions under different wavelengths of illumination.

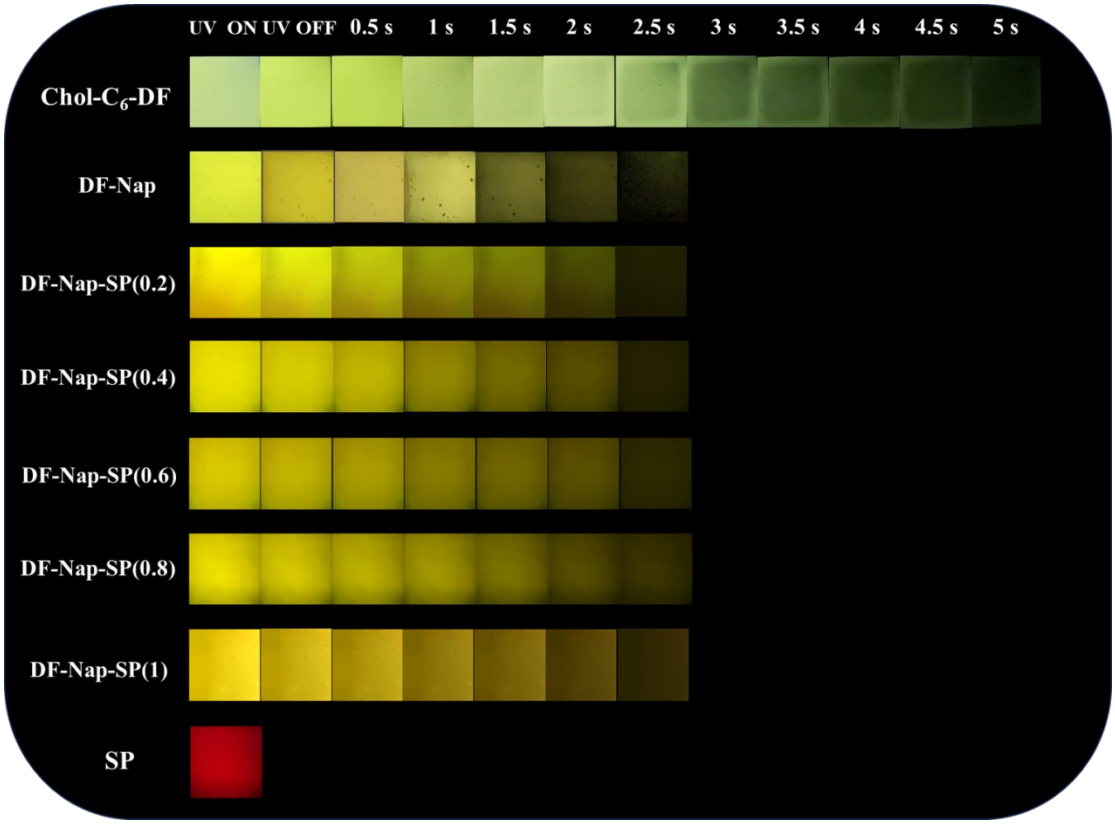

Figure S8. Photographs of Chol-C_6-DF, DF-Nap and DF-Nap-SP(n) taken under a 365 nm UV lamp on and off (none of the samples were previously irradiated with 365 nm light).

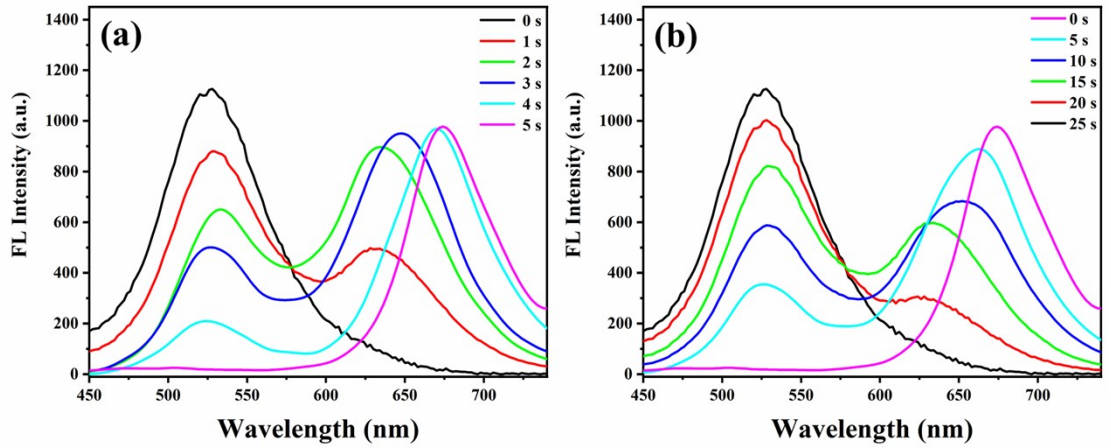

Figure S9. Emission spectra of SP film under irradiation with 365 nm light (a) and subsequent exposure to 470 nm light (b) (λ_{ex}=380 nm).

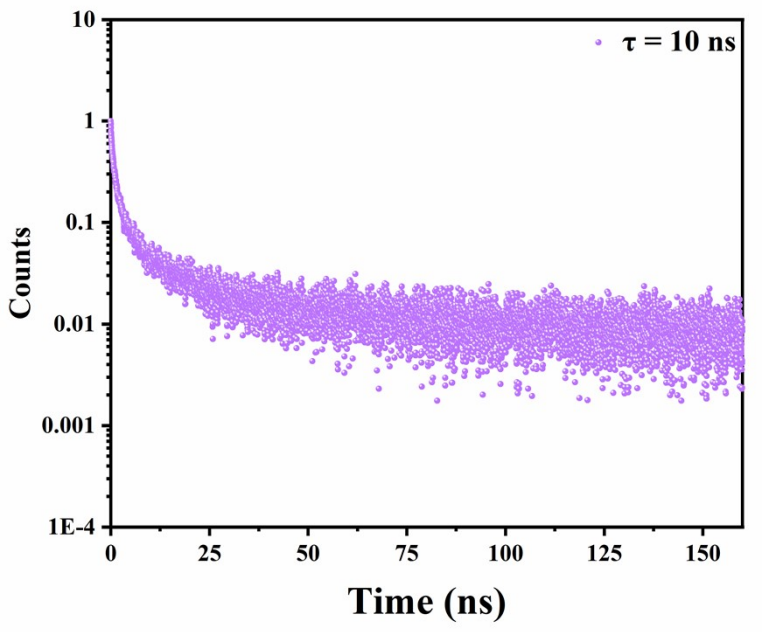

Figure S10. The lifetime decay curve of SP film at 680 nm (λ_{ex}=580 nm).

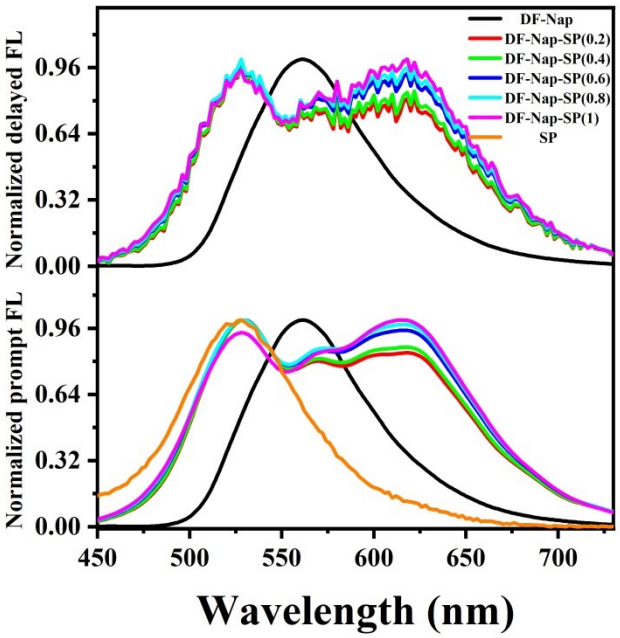

Figure S11. The normalized prompt and delayed emission spectra (T_d=0.2 ms) of SP, DF-Nap and DF-Nap-SP(n) with different doping amount of SP before 365 nm UV irradiation.

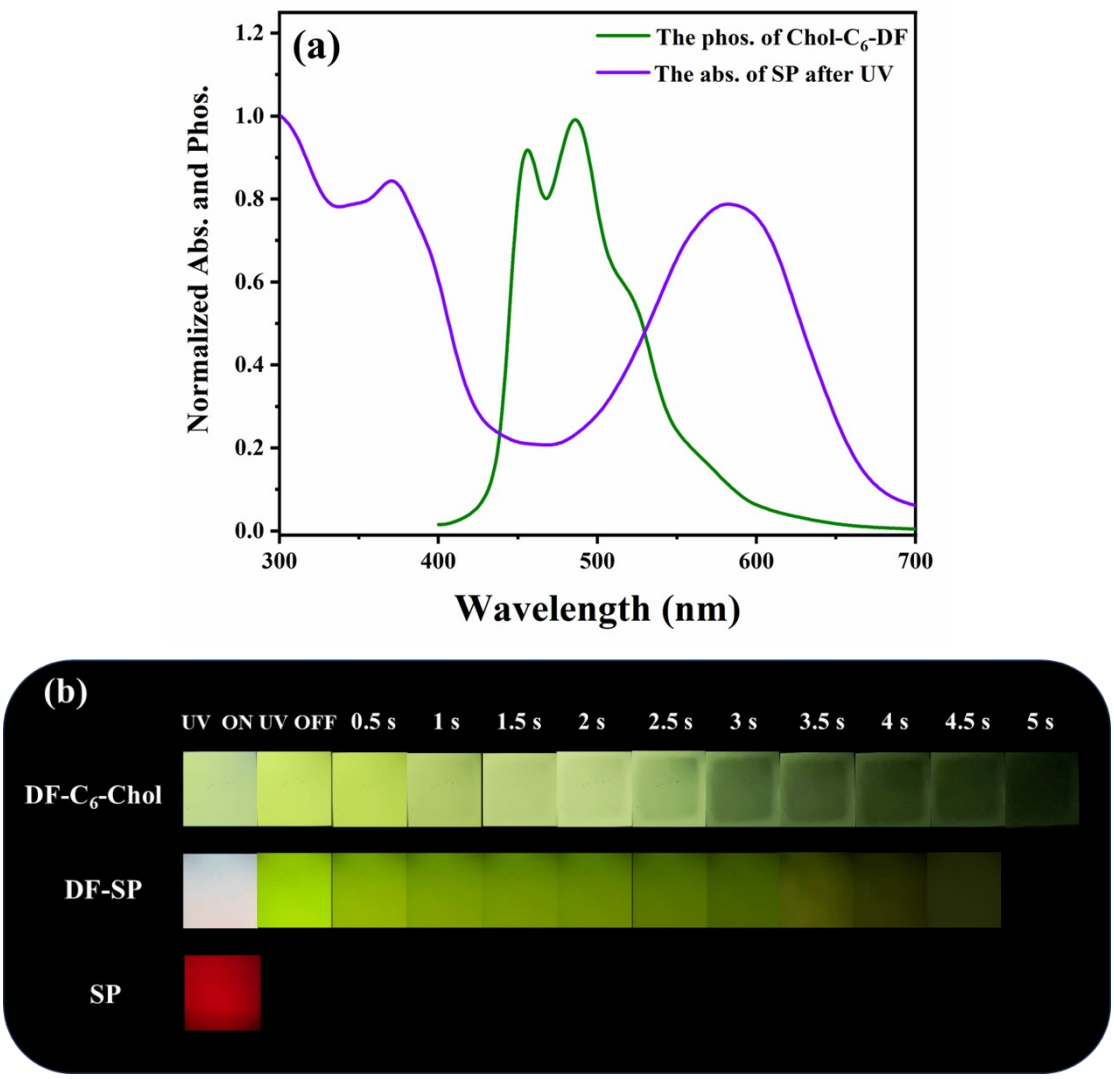

Figure S12. (a) Phosphorescent emission spectrum of Chol-C_6-DF film (λ_{ex}=380 nm) and the absorption spectrum of SP film after 365 nm UV irradiation. (b) Photographs of Chol-C_6-DF, DF-SP and SP after 1 min of illumination taken under a 365 nm UV lamp on and off.

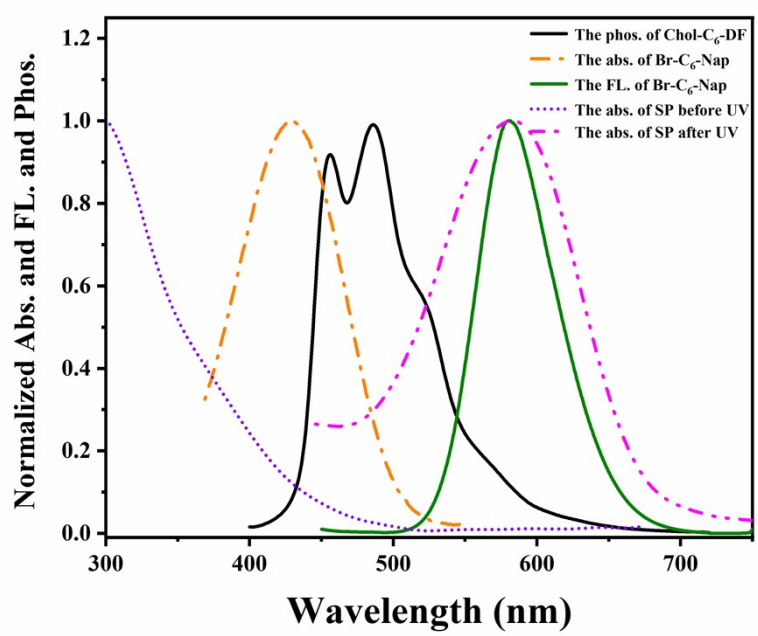

Figure S13. The absorption spectra of Br-C_6-Nap film, SP film before and after 365 nm UV irradiation, phosphorescent emission spectrum of Chol-C_6-DF film (λ_{ex}=380 nm) and fluorescence emission spectrum of Br-C_6-Nap film (λ_{ex}=425 nm).

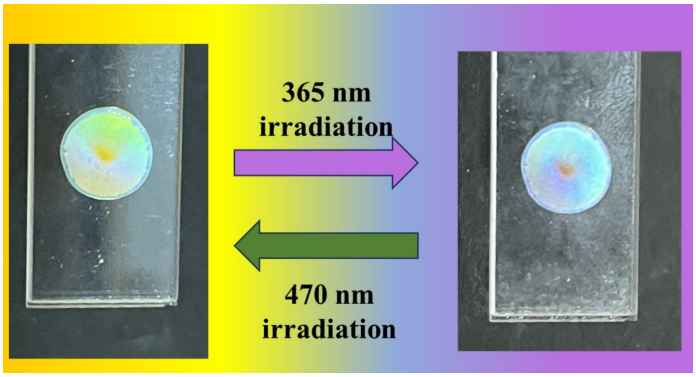

Figure S14. The structural color change of DF-Nap-SP(0.4) before and after illumination.

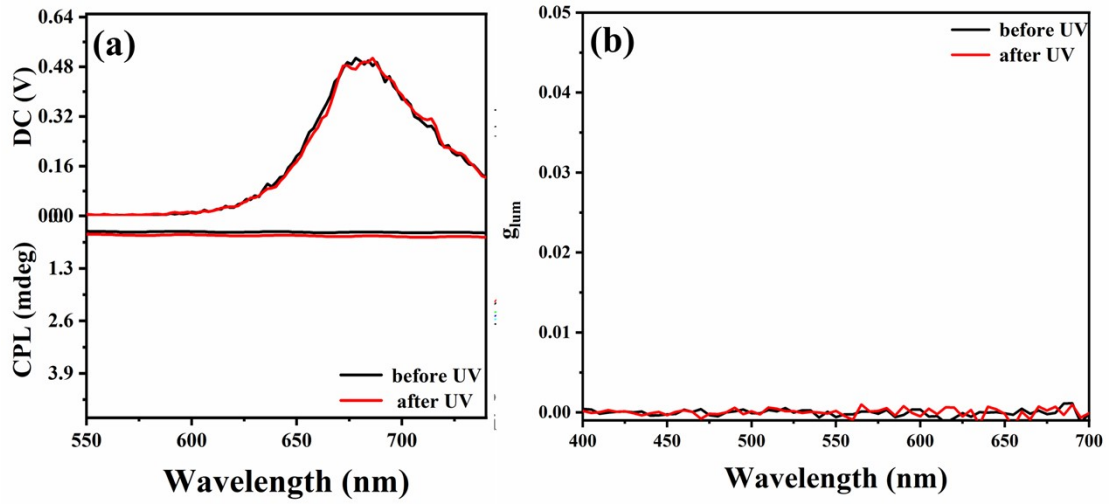

Figure S15. (a) The CPL spectra and (b) the corresponding g_{lum} spectra of SP before and after 365 nm UV irradiation (λ_{ex}=380 nm, film thickness=100 um).

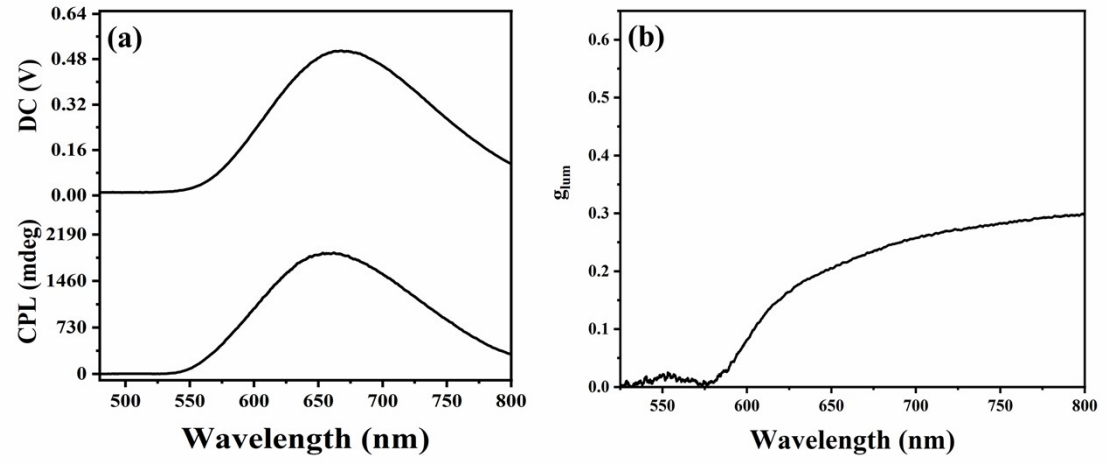

Figure S16. (a) The CPL and synchronous emission spectra of DF-Nap-SP(0.4) thin film (λ_{ex}=380 nm, film thickness=5.6 um). (c) The corresponding g_{lum} spectrum of DF-Nap-SP(0.4).

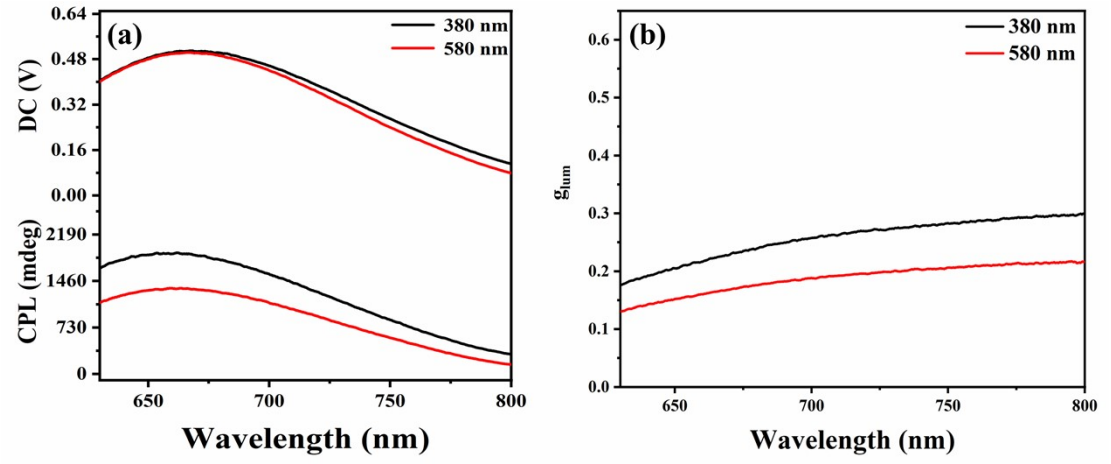

Figure S17. (a) The CPL spectra and synchronous emission spectra of the 5.6 μm DF-Nap-SP(0.4) film under different excitation wavelengths. (b) The corresponding g_{lum} spectra.

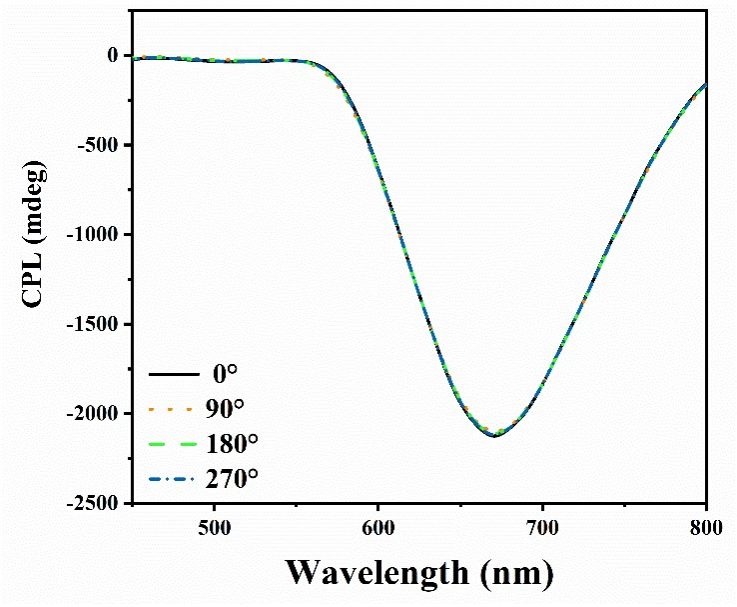

Figure S18. The CPL spectra of DF-Nap-SP(0.4) at different rotation angle (film thickness=100 um, λ_{ex}=380 nm).